Effect of polymer network on thermodynamic stability and switching behavior of the smectic-C^*_α phase

Magdalena Knapkiewicz,[1] Mariola Sądej,[2] Wojciech Kuczyński,[1] and Adam Rachocki[1,*]
[1]*Institute of Molecular Physics, Polish Academy of Sciences, M. Smoluchowskiego 17, 60-179 Poznań, Poland*
[2]*Faculty of Chemical Technology, Poznan University of Technology, Berdychowo 4, 60-965 Poznań, Poland*
(Received 17 May 2017; revised manuscript received 12 August 2017; published 8 November 2017)

A polymer-stabilized liquid crystal based on 4′-(octyloxy)biphenyl-4-carboxylate 2-fluoro-4-((octyl-2-yloxy)carbonyl)phenyl (D16) and 1,6 hexanediol diacrylate as a monomer was prepared by *in situ* photopolymerization. The selected antiferroelectric liquid crystal contains a fast-switching smectic C^*_α phase (SmC^*_α), and the influence of the polymer network on the thermodynamic stability of this phase and its switching behavior under applying time-dependent electric field were studied. Using dielectric spectroscopy and polarizing microscopy, the liquid crystal materials were characterized, and subsequently with the use of the reversal current method (RCM) the current response, especially from the SmC^*_α phase was carefully analyzed. The current response is complex and also depends on the neighboring liquid crystal phases. In the liquid crystal-polymer system, as well as in the liquid crystal-monomer mixture, a significant shift of the temperature range of the SmC^*_α phase toward lower temperatures was observed; however, the thermodynamic instability related to the transformation to the crystalline phase was also noted and characterized. Because of the fuzzy phase transitions detected in the liquid crystal-polymer system by dielectric spectroscopy and also because of the lack of the characteristic dielectric signature of SmC^*_α after polymerization, we proposed the use of the RCM, as a complementary one, to identify the SmC^*_α phase even in such complex materials.

DOI: 10.1103/PhysRevE.96.052702

I. INTRODUCTION

Liquid crystals (LCs) are unusual materials that exhibit many unique and attractive properties, following from the ability to combine the characteristics of solids and fluids. For instance, they show long-range ordering like crystals and simultaneously are flowable like liquids, they reveal optical activity (their molecules cause rotation of the polarization plane of light) and ferroelectric properties (the flowable ferroelectrics can be found only among LCs). Nowadays, they are commonly used in fast-switching electro-optical devices. The LC materials characterized by a very short reaction time on application of the electric field are successfully used in photonics. The photonics combines the achievements of optics, computer science, and electronics, and most importantly, it is focused on utilization of light for the benefit of mankind. LC-based devices (among others, logic gates, optical shutters, diodes, and transistors, etc.) are used to construct the photonic integrated circuits and optical computer prototypes [1–4]. Combinations of unique features of LC phases, especially SmC^*_α one, with specific properties of polymer matrices allow obtaining a new generation of liquid crystal-polymeric composite materials. The study presented by us fits squarely into the current search for new composite materials to meet the needs of modern technology.

According to the nomenclature used by the Liquid Crystal Society, the materials that contain only the ordinary chiral smectic C phase (SmC^*) are called ferroelectric liquid crystals (FLCs), whereas antiferrolectric liquid crystals (AFLCs), besides SmC^*, include other variations of the chiral smectic C phases (i.e., SmC^*_A, SmC^*_α, SmC^*_β, SmC^*_γ). This is the original Fukuda school nomenclature [5]. Among different phases of AFLCs, the SmC^*_α one is particularly interesting because its switching time is of the order of microseconds [6–9]. The switching time is the parameter that characterizes the switching electro-optical devices and reflects the change in the optical response to the applied electric field. It is inversely proportional to the magnitude of the applied field as well as ferroelectric spontaneous polarization, and proportional to the rotational viscosity that is the characteristic constant of the material [10].

On the basis of x-ray studies, the structure of SmC^*_α was proposed in 1999 [11,12]; nevertheless, other molecular models are also considered to describe this phase [13,14]. As shown in Refs. [11,12] the SmC^*_α phase is defined by a few-layered clock-like structure formed by the molecules that, on average, are tilted by the angle (θ) to the layer normal, and similarly to SmC^*, the tilt direction is changed from layer to layer forming a helix. The significant difference, with respect to the SmC^* phase, is that the pitch of helix containing only a few molecular layers is relatively shorter in SmC^*_α. The angle θ in SmC^*_α (typically of the order of a few degrees) is also very small when comparing that in the chiral smectic-C family (usually about 30 degrees [5]). As a consequence of the small tilt angle, and because of lower viscosity of the SmC^*_α phase in comparison to SmC^* within the material, the switching time in SmC^*_α may be shorter than a few microseconds, while for instance in the SmC^* phase it is ten times longer [6]. Another important issue is that the SmC^*_α phase commonly exists in a rather narrow temperature range of only a few centigrades. Although this disadvantage limits the use of this phase in practical application, some successful attempts to widen the temperature range of the SmC^*_α phase using chiral dopants and photopolymerization method were reported [15,16].

Despite some limitations of the SmC^*_α phase one can expect that in the near future polymer stabilization of this phase will attract growing interest of scientists for several reasons. (1) The SmC^*_α phase is characterized by fast response time and low rotational viscosity [6]. (2) The temperature range of some LC phases (i.e., blue phases) can be successfully extended

*adam.rachocki@ifmpan.poznan.pl

using photo-reactive monomers [17] and a great number of applications of polymer stabilized blue phases have been found [18–20]. (3) Archer *et al.* have mentioned that the presence of polymer network reduces the effective viscosity and the response times of polymer-stabilized FLCs (PSFLCs) become shorter, even when compared to those observed for the neat ferroelectric material [10,21]. (4) Labeeb and coworkers have reported that they have been able to extend the temperature range of the SmC^*_α phase from 3 to 39 °C [16].

The study reported in this paper is focused on an important problem concerning difficulties in polymer stabilization of the SmC^*_α phase. The polymer stabilization of the SmC^*_α phase is understood as a creation of the polymer network within the SmC^*_α phase. This stabilization is aimed at the phase protection from degradation with time as well as at the widening of the phase temperature range in relation to the temperature range of SmC^*_α phase in the absence of the polymer network. We have tested *in situ* photopolymerization on the LC material with relatively long temperature range of existence of the phase considered [22,23]. We describe the used preparation and pay attention to issues which are important for the researches who are interested in further development of this area. Especially, the changes in thermodynamic stability of LC phases induced by addition of a monomer and polymer dopant, or experimental problems with proper detection of the temperature range of SmC^*_α are considered.

II. MATERIALS AND METHODS

The AFLC material of 4′-(octyloxy)biphenyl-4-carboxylate 2-fluoro-4-((octyl-2-yloxy)carbonyl) phenyl was purchased from AWAT Company (Warsaw, Poland). This compound, henceforth denoted as D16, is composed of rodlike molecules of the structural formula presented in Fig. 1. The central part of these molecules consists of an aromatic core containing three benzene rings. The functional group that is attached to this core makes the molecular chirality center (marked with an asterisk in the figure). Both sides of the elongated molecule are terminated by aliphatic chains.

On the basis of the second harmonic electrooptical spectra analysis, the following phase sequence of D16 was determined on cooling [23]:

$$\text{Cr}\,28\,^\circ\text{C}\ SmC_\gamma{}^*\,47\,^\circ\text{C}\ SmC_\beta{}^*\,51\,^\circ\text{C}\ SmC_\alpha{}^*$$
$$63\,^\circ\text{C}\ \text{SmA}\,119\,^\circ\text{C}\,\text{Iso}.$$

Both the crystallization temperature (Cr) and the temperature of the Iso-SmA phase transition were determined by differential scanning calorimetry (data not shown here). However, the crystallization process can be initiated even at higher temperatures, as will be discussed later in this paper.

The main reason for choosing this compound for further investigation was a wide temperature range of the SmC^*_α phase which exists over a range of 12 °C. The SmC^*_α phase is present along with the SmC^*_β, SmC^*_γ, and SmA phases. The SmC^*_β, SmC^*_γ are subgroups of the C-type smectics, which have a four-layer and three-layer clock structure, respectively. The SmA phase is nontilted liquidlike smectic type, in which the molecules are oriented on average in parallel to each other and form the layers with the average long molecular axis parallel to the layer normal.

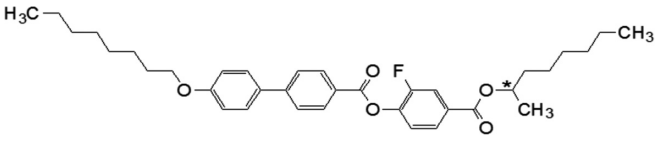

FIG. 1. Structural formula of liquid crystal D16 molecule.

The dielectric and optical measurements, as well as those using the reversal current method, were made on the commercial measuring cells (E.H.C. Company, Ltd. in Tokyo, Japan) composed of two glass plates separated by an epoxy 10-μm spacers and coated with a thin layer of indium tin oxide (ITO) and rubbed polyimide, providing the electrodes and surfaces to promote planar alignment of the LC molecules, respectively. The cells were filled with LC systems and were mounted in a modified Mettler FP 82 HT hot stage. The temperature of the samples was controlled by the home-made temperature controller. The temperature stability was better than 0.05 °C.

The dielectric spectroscopy (DS) measurements were performed using an Impedance Analyzer 4192A from Hewlett-Packard. A sinusoidal measuring voltage of 0.5 V and frequency of 440 Hz was applied. Temperature dependencies of the electric permittivity were collected both on heating and cooling cycles, besides the isothermal changes in the permittivity as a function of time were recorded.

The current responses in the reversal current method (RCM) were recorded using a home-made system that consisted of modified DDP (Diamant, Drensk, and Papinsky) bridge, a voltage generator with an amplifier (FLC Electronics), and an oscilloscope connected to a computer. A triangular voltage of amplitude 80 V (peak-to-peak) and frequencies of 10 and 100 Hz were applied. The experimental data were recorded only on cooling cycles.

Standard polarizing-microscope observations were carried out using a BX-53F Olympus microscope equipped with a digital camera. The samples' textures were recorded on cooling cycles, as well as a function of time keeping isothermal conditions.

The photopolymerization reaction were carried out for LC-monomer mixture composed of D16 and small amount of 1,6 hexanediol diacrylate (HDDA) as the aliphatic monomer (5 wt.%), and a minute quantum (1 wt.%) of 2,2-dimethoxy-2-phenylacetophenone (Irgacure 651) as the photoinitiator. The mixture was heated up to the isotropic phase and then inserted into measuring cell. The filled cell was cooled at a rate lower than 1 °C/min down to the temperature at which the polymerization was initiated in the SmC^*_α phase at 46 °C. Previously, this temperature was determined by RCM. The photopolymerization was carried out for 50 min by a UV lamp (VP-60, Poland) operating with the power of 180 W and the power density of approximately 11 mW/cm^2 detected at the surface of the irradiated sample.

III. RESULTS AND DISCUSSION

A. Characterization of liquid crystals

1. Phase sequence characteristics

Accurate identification of liquid crystal phases and phase transitions can be achieved by a number of experimental

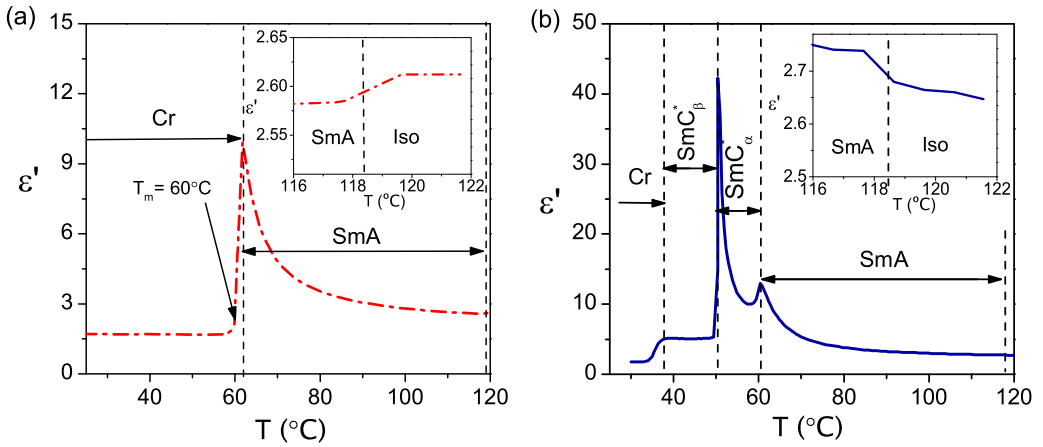

FIG. 2. Thermal hysteresis of the temperature dependency of the electric permittivity in neat D16 at 440 Hz taken on heating (a) and cooling (b).

methods. Quite often more than one method is needed to recognize all phase transitions within a given substance. One of the most commonly used techniques in this field is dielectric spectroscopy (DS) which usually provides valuable information on the phase sequence characteristic of a given LC system. The results obtained from DS are a good starting point for further analysis.

Figure 2 presents the obtained temperature dependencies of the real part of permittivity, $\varepsilon'(T)$, for D16. The experimental data were independently recorded both on cooling from isotropic phases (Iso) and on heating from crystalline ones (Cr)—Figs. 2(a) and 2(b), respectively. On cooling the Iso-SmA phase transition is manifested by a rather smooth change in permittivity close to 119 °C [see the insert in Fig. 2(b)], whereas the SmA-SmC^*_α and SmC^*_α-SmC^*_β phase transitions are reflected by sharp peaks clearly visible at 60 °C and 50 °C, respectively (see also Table I). A significant increase in ε' observed as the temperature decreases close to the SmA-SmC_α phase transition is caused by anomalous behavior of the elastic constant responsible for the increase of the amplitude fluctuations of the order parameter, which critically slow down near the phase transition temperature (*soft mode*). In contrast to SmA, the SmC^*_α phase exhibits a helical structure in which a phase distortion mode (*Goldstone mode*) associated with the changes in azimuthal variations of the tilt direction is clearly prominent in the $\varepsilon'(T)$ dependence as the increase in the ε' magnitude in the temperature range of 50–60 °C. In SmC^*_β the polarization vanishes and a rapid decrease in the ε' magnitude is observed at the temperature corresponding to the SmC^*_α/SmC^*_β phase transition. The SmC^*_β phase can easily be recognized among other LC phases of the chiral smectic-C family because of a low-frequency dielectric response (a small value of ε') reflecting the mesoscopic polarization zero. The mesoscopic polarization is defined as a vector sum of spontaneous polarization vectors of different layers in the repeating unit of the phase, whereas the presence of the helix results in a residual macroscopic polarization of the entire sample.

The SmC^*_γ phase has not been detected in the dielectric response below the SmC^*_β phase (any characteristic increase of ε' was not observed below the SmC^*_β phase). Nevertheless, the characteristic decrease in the electric permittivity is detected below 39 °C and can be associated with the onset of the crystallization process. Unlike on cooling, on heating of D16 from room temperature up to the isotropic phase only the melting point (T_m) of the crystal at 60 °C is clearly marked, above which the SmA phase exists up to approximately 119 °C at which the SmA/Iso phase transition is observed. It is important to emphasize that in contrast to the observations on cooling, no phases with a helical structure are detected in D16 on heating.

The complementary observations of textures were carried with the polarized microscope to confirm the presence of the SmC^*_α and SmC^*_β phases in D16. The typical fan-shaped focal conic textures of both phases are presented in Fig 3. For SmC^*_α the characteristic structural elements are the "ripples" visible along the focal conic domains [Fig. 3(a)], whereas characteristic of SmC^*_β are the "stripes" that appear across the

TABLE I. The phase sequences in neat D16, D16/HDDA, and PSD16 determined by dielectric spectroscopy on heating and cooling.

Material		**Phase sequence**
D16	Heating	Cr 37.5 °C SmC^*_β 50 °C SmC^*_α 60 °C SmA 118.3 °C Iso
	Cooling	Cr 62 °C SmA 118.3 °C Iso
D16/HDDA (mixture)	Heating	Cr 61.2 °C SmA 115.7 °C Iso
	Cooling	# 43.5 °C SmC^*_α 52 °C SmA 115.7 °C Iso
PSD16	Heating	Cr 61 °C SmA 115.1 °C Iso
	Cooling	# 38.5 °C SmC^*_α 43 °C SmA 115.1 °C Iso

# denotes the temperature region with possible coexistence of LC and crystalline phases; the crystallization temperature was not determined in these cases.

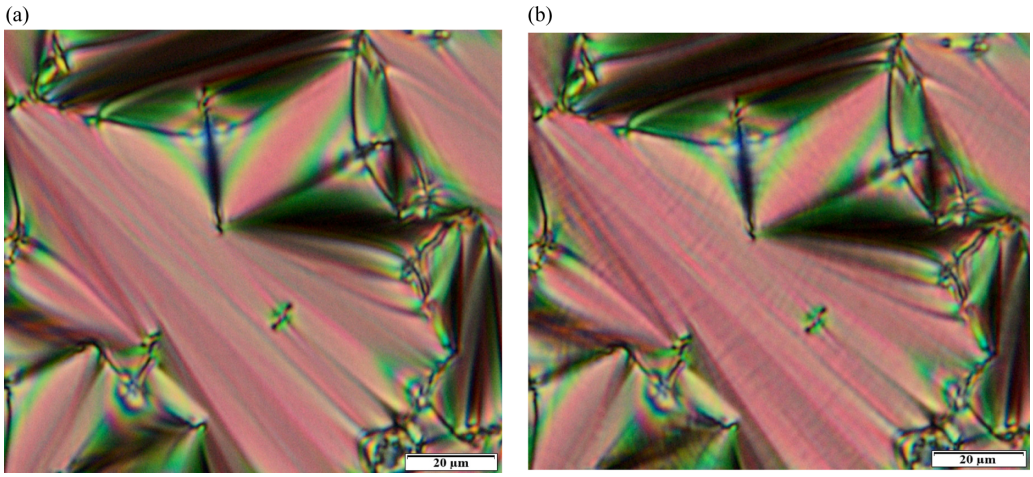

FIG. 3. Textures recorded for neat D16 in the SmC^*_α phase at 58 °C (a) and in the SmC^*_β phase at 48 °C (b) with the polarized microscope.

domains [Fig. 3(b)]. The "stripes" are characteristic of any phase with a pitch longer than wavelength of visible light [5].

2. Thermodynamic stability investigation

One of the most important pieces of information obtained from the DS studies is that some of LC phases were found above and some of them below the melting temperatures characteristic of the materials under investigation. It is well known that LC phases present in temperatures above the melting point are called enantiotropic ones. They are thermodynamically stable and their existence is independent of the direction of temperature changes. The data shown in Fig. 2 indicate that the enantiotropic phase in D16 is only the SmA one. On the other hand, on cooling and below melting point the so-called monotropic (i.e., supercooled) LC phases were detected. The monotropic phases do not show the lowest free energy for specific temperature and pressure. They defined as metastable ones (i.e., kinetically stable but thermodynamically unstable) exists only for a specified period of time. On the basis of the results presented in Fig. 2 we expect that both SmC^*_β and SmC^*_α are metastable phases. To obtain more detailed information on possible instability of these phases, we performed additional electric permittivity studies.

The permittivity of D16 as a function of time at given temperatures (40, 46, 48, and 52 °C) is presented in Fig. 4(a). For each of the selected temperatures the measuring procedure was as follows: at first the sample was heated up to the isotropic phase and then cooled at the rate of 1 °C/min down to the temperature at which the ε' data were recorded with time. When the material fully crystalized, it was cooled down to room temperature to start the next series of measurements at a subsequent temperature. From the data collected in Fig. 4(a) we were able to assess the characteristic lifetime of the metastable states that depends on the LC phase type and temperature conditions. The lifetime, t_l, we define as a period in which the maximum and constant value of the ε' characteristic of particular temperature is maintained in the system. After this time the onset of the crystallization process is observed. The longest t_l, i.e., longer than 7 h, was found for the SmC^*_α phase at 52 °C, while at the lower temperatures, which correspond to the SmC^*_β phase, the t_l times were much shorter. For instance, at 48 °C the crystallization process is initiated effectively after approximately 20 min, while at 40 °C it starts uncontrollably.

It should be emphasized that a relaxation of the metastable state toward the stable one requires an activation to overcome an energy barrier and thus a more time and higher energy is needed by the system to achieve the equilibrium state (to crystallize) at higher temperature. With decreasing temperature the efficiency of the crystal nucleation increases [24] and when the number of the crystallization nuclei crosses some critical level then the avalanche process of crystallization takes place. The nucleation efficiency depends not only on temperature but also on other external stimuli which can be provided in the form of an electric field or mechanical vibrations. The estimated herein lifetimes do not have exact physical meaning because it is difficult to unambiguously define them for a given phase, especially, if they vary depending on the experimental method. Nevertheless, they allow a qualitative view on the metastability observed in the systems under investigation.

It should be mentioned that the metastability described above is a common phenomenon observed in LCs. Monotropic phases were found in at least 37 compounds from over 100 reviewed by Vorländer [25]. Thus, in terms of phase stability a proper verification of the material is required, particularly due to its entrapment in a polymer matrix. In this paper, we focus mainly on the polymer-stabilized of the SmC^*_α phase, and the crucial question arises, how the presence of the polymer guest affects the physical properties of this phase including its thermodynamic stability.

B. Photopolymerization effect

1. The phase sequence characterization

The LC/polymer system based on D16 as host molecules, and HDDA monomer as a guest dopant was prepared. Prior to photopolymerization, the initial LC/monomer mixture (D16/HDDA) was prepared and after solvent removal the dielectric measurements were performed on heating [Fig. 5(a)] and cooling [Fig. 5(b)] to determine possible changes in the characteristics of the phase transitions observed in the mixture. As can be seen in Fig. 5 and in Table I, the addition of guest

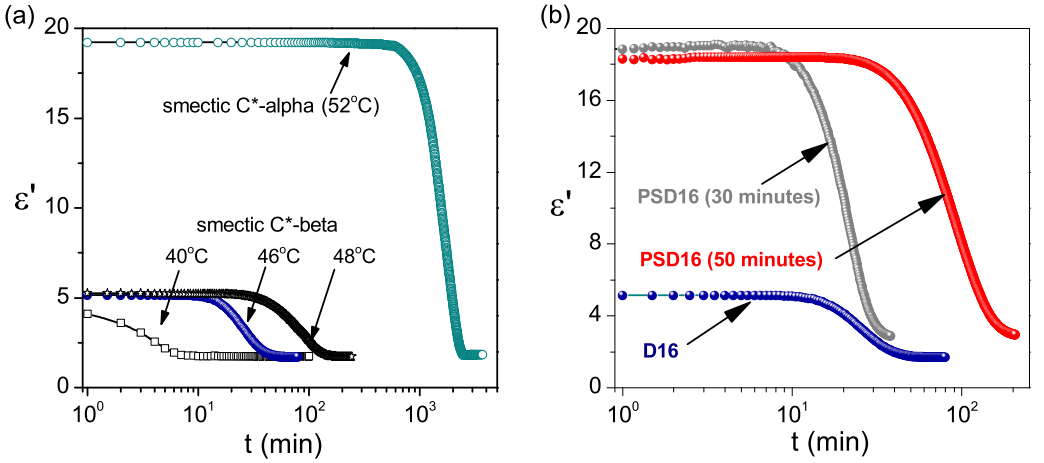

FIG. 4. Kinetics of the crystallization process in neat D16 at 40, 46, 48, 52 °C (a) and in PSD16 at 46 °C (after 30 and 50 min of polymerization) in comparison to neat D16 at 46 °C (b).

molecules to the host LCs results in a change in LC phase transition temperatures.

For D16/HDDA a significant shift in the temperature range of the SmC^*_α phase toward lower temperatures is evident [Fig. 5(b)]. On the other hand, the results obtained on heating [Fig. 5(a)] indicate that the presence of the monomer has no significant influence on the change in the melting temperatures of the crystalline phases.

Taking into account that in the LC-monomer mixture the temperature range of the SmC^*_α phase is shifted, photopolymerization reaction was carried out at 46 °C within the SmC^*_α phase for 50 min. The kinetics of the crystallization process in the mixture at the temperature chosen for the polymerization was not studied. We assume that the stability of the SmC^*_α phase within polymerization time can change to a certain extent. Nevertheless, before polymerization the presence of the SmC^*_α phase at this temperature was confirmed using reversal current method, as it will be mentioned latter. One can also consider that during long time of polymerization the crystallization process may be initiated, and thus a coexistence of the SmC^*_α and crystal phases is possible both at the polymerization stage of the mixture as well as in the fabricated polymer-stabilized LC. The newly synthetized LC-polymer system was then characterized by dielectric spectroscopy in the analogous way as LC-monomer mixture or neat LC before.

As shown in Fig. 5(a) the presence of the polymer network only slightly affects the melting points of the materials, however, a further change in the temperature range of the SmC^*_α phase in PSD16 takes place and it is now shifted towards lower temperatures down to 40–46 °C [see Fig. 5(b)]. Above SmC^*_α, the SmA phase appears, whereas below SmC^*_α a coexistence of LC and solid phases is possible on cooling. In turn, on heating only SmA exists above the melting point in the temperature range of 46–119 °C.

Although the effect of polymerization is evident, the SmC^*_α phase seems to be still thermodynamically unstable. Therefore, additional isothermal dielectric measurements were performed. The results obtained at 46 °C are presented in Fig. 4(b). The longest lifetime, t_1, was found for PSD16 polymerized for 50 min, whereas the shortest one—for PSD16 polymerized for 30 min. Furthermore, the t_1 for PSD16 polymerized for 30 min is even shorter than that observed for neat D16 at 46 °C. It can be explained by partially polymerized system after shorter polymerization time. Then monomers

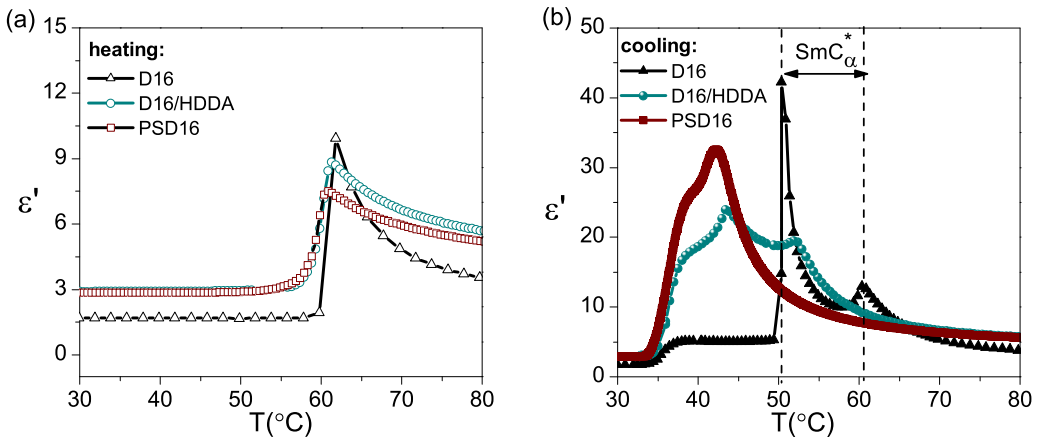

FIG. 5. Thermal hysteresis of the temperature dependencies of the electric permittivity in D16, D16/monomer, and PSD16 on heating (a) and on cooling (b) cycles.

form dimers, trimers, or even oligomers but the polymer network is not fully formed. Extension of the polymerization time to more than 50 min has no effect on the thermodynamic stability of the system. Thus, it can be concluded that the effective polymerization (for about 50 min) improves the stability of the polymer-LC system over that of neat LC. However, generation of polymer network in the SmC^*_α phase also results in a shift of the phase temperature in which this phase occurs toward lower temperatures at which the process of nucleation is more effective. From the point of view of applications, this result indicates that it may be relatively difficult to fabricate the thermodynamically stable SmC^*_α phase in a broad temperature range by polymerization. In literature we have found only one paper concerning the broadening of the temperature range of the SmC^*_α phase by photopolymerization [16], which fortunately was not monotropic phase.

It seems also interesting to compare the difference in electric permittivity in the temperature range of the SmC^*_α phase between the LC-polymer system and that observed in neat LCs. Analysis of the behavior of the temperature dependencies of permittivity in Fig. 5(b), reveals that the dielectric constant is lower in PSD16 than that in D16, when comparing the low-temperature regions of SmC^*_α [see full triangles and full squares in Fig. 5(b)]. The decrease in ε' observed earlier in other polymer-stabilized smectic phases was explained by the fact that the presence of polymeric structures suppresses the helix distortion mode [26]. This suppression can be understood taking into account the elastic coupling between the polymer network and LC molecules, which reduce collective molecular fluctuations. The effect of the polymer network on the dielectric properties in polymer-stabilized FLCs was described in details by S. Kaur *et al.* [27]. In PSLC and in the LC-monomer mixture prepared by us, the LC phase transitions are observed in much wider temperature ranges then those in neat LC. It should be emphasized that similar effects are characteristic of LC materials with addition of impurities. However, as a result of polymerization the presence of the polymer network affects the value of ε' and the characteristic dielectric response of SmC^*_α disappears. Consequently, it is difficult to unambiguously confirm the existence of SmC^*_α by dielectric spectroscopy. For this reason we tackled the problem of identification of the SmC^*_α phase in the polymerized materials by the reversal current method (RCM).

2. *Switching behavior of the* SmC^*_α *phase*

According to literature in the high-temperature region of the SmC^*_α phase, the sample under RCM conditions switches similarly as the surface-stabilized SmC^*, while the switching character in the low-temperature range is similar to that of the SmC^*_A placed in a thin ($\sim$2 μm) planar measuring cell [28–32]. Obviously the current response from SmC^*_α observed by the reversal current method only mimics the SmC^*_A; however, it has a completely different nature and will be discussed below [5].

It is also known that a single peak observed in the current response is characteristic of the surface-stabilized SmC^*. In RCM the current is recorded while the voltage applied is linearly changed over time from the maximum positive value U_+ to the minimum negative U_-. Initially, for U_+, all molecules are tilted in the same direction with respect to the layer normal, and the tilt is defined by the angle θ. The orientation of these polar molecules is forced by the strong electric field. Every single smectic layer of the C^* phase has a nonzero spontaneous polarization, and the direction of the polarization can be controlled by the electric field. When the sign of the voltage is changed from U_+ to U_-, the molecules are switched between the initial state characterized by the tilt angle θ to the final one with $-\theta$. The sense of the polarization vector is also changed to the opposite one.

For the thin sample ($\sim$2 μm) of SmC^*_A, typically, one can distinguish two peaks in the current response [5]. These symmetrical peaks with similar integral intensities appear on both sides of zero voltage. Applying U_+ all molecules are tilted by the angle θ. The first peak is related to the molecules from every second layer which change their orientation from the initial (θ) to the final state ($-\theta$). The second peak occurs when the molecules in the other layers change their orientation in a similar way. According to the literature helical order on a micrometer scale is absent due to the plates covered by alignment layers [32]. When no field is applied, usually the smectic directly returns to the antiferroelectric (commensurate aniferroelectric, anticlinic) state [5].

In the high-temperature region of SmC^*_α the two peaks are also observed in the current response even if the thickness of the measuring cells is small. However, these peaks reflect the winding and unwinding process of the helical structure. The initial orientation of the molecules (applying U_+) is such that all of them are tilted by the angle θ, the helical structure is destroyed, and the polarization vector is aligned to the electric field direction. If the electric field effect is low enough with respect to the intermolecular interactions, the helical winding process occurs and the helical structure is created. As a function of time the voltage decreases to zero and then increases with the opposite sign. The helical structure exists as long as the voltage applied does not exceed a negative critical value. Above this voltage the helical unwinding process starts and the helical structure of the SmC^*_α phase is destroyed again. Finally, all LC molecules are tilted by the angle $-\theta$.

The current response from the SmC^*_α phase becomes more complex with decreasing temperature. According to literature, the lower the temperature the more molecules switch like surface-stabilized SmC^* and the less of them switch through the helical structure winding and rewinding [33]. However, in the low-temperature range of SmC^*_α another type of switching, dependent on the phase which occurs below SmC^*_α on cooling. The results obtained in D16, D16/HDDA mixture and PSD16 by RCM are presented in Fig. 6.

In D16 the SmC^*_β phase exists in lower temperatures than the SmC^*_α one. The current response from SmC^*_β clearly depends on frequency of the applied electric field. In neat D16 three peaks characteristic of SmC^*_β are observed at 50 °C when applying voltage at 10 Hz [Fig. 6(a)], while only one peak is observed at the same temperature at 100 Hz [Fig. 6(b)]. Thus, as can be seen, the switching behavior is independent of frequency in the high-temperature range of SmC^*_α, while in the low-temperature region the current response depends on frequency. This observation is characteristic of the SmC^*_α phase when the neighboring phase is SmC^*_β.

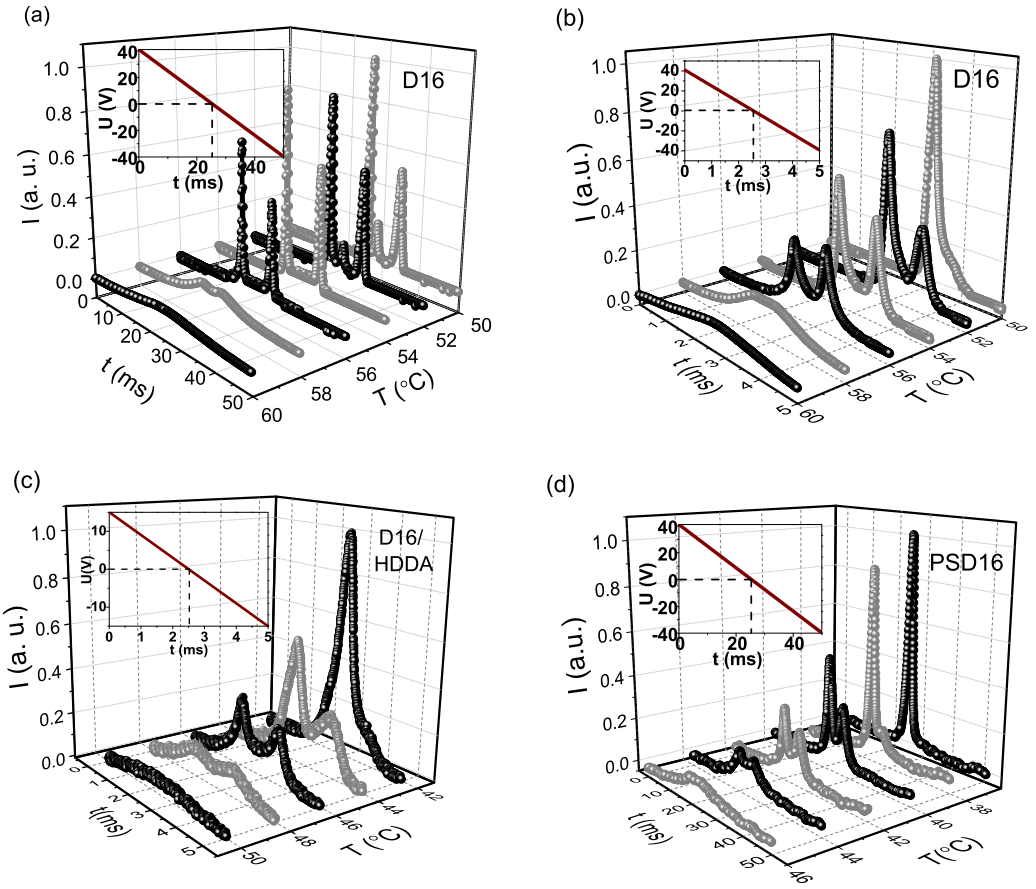

FIG. 6. The current response from the SmC^*_α phase in D16 at 10 Hz (a) and 100 Hz (b), the mixture of D16/HDDA at 100 Hz (c) and PSD16 at 10 Hz (d) recorded with reversal current method (RCM) on cooling cycles; the applied voltage was changed linearly from 40 to −40 V for (a), (b), and (d), and from 15 to −15 V for (c).

The current response recorded for the systems under investigation before and after polymerization is presented in Figs. 6(c) and 6(d), respectively. Especially, the data collected for the mixture (D16-HDDA) confirm the existence of the SmC^*_α phase at 46 °C, i.e., at the temperature wherein the photopolymerization process was initiated.

In PSD16 in the temperature region below SmC^*_α the coexistence of LC and crystalline phase takes place (see Table I). There are two premises suggesting that the LC phase is SmC^*. First, the phase switches as SmC^*-high, a slender peak is observed in Fig. 6(d) at 36 °C applying 10 Hz. Second, according to literature, the SmC^*_β phase exists only in very pure materials (even optically pure ones); in other cases, the phase is changed to SmC^* [34]. Unfortunately, in the considered temperature region [Fig. 4(b)] the value of permittivity is smaller than that in SmC^*_α. This unexpected behavior is most likely caused by the presence of the crystalline phase. Nevertheless, Fig. 6(d) proves that the SmC^*_α phase still exists in PSD16. The current responses observed in D16 and in PSD16 at 10 Hz [Fig. 6(a) and Fig. 6(d)] look different at low-temperature regions, because in this temperature regions the LC phase coexistence takes place. In D16 SmC^*_α coexists with SmC^*_β [Fig. 6(a), 52–56 °C], whereas in PSD16 the SmC^*_α phase probably coexist with the SmC^* phase [Fig. 6(d), 36–41 °C].

The reversal current method is often used to determine the temperature range of the SmC^*_α phase. However, the interpretation of the results obtained with this method can be quite complicated because two peaks in the current response are observed like in the SmC^*_α phase, as well as in the SmC^*_A [24], de Vries smectics [35], and even in SmC^* with ultrashort helical pitch [36].

In contrast to the dielectric spectroscopy, RCM is an alternative experimental method alternative to x-ray scattering, if one can determine the existence of "pure" phase, i.e., without any phase coexistence. In particular it allows identification of the temperature region of the LC phase in which the molecules switch only through winding and unwinding helical superstructure as in the SmC^*_α phase. It is important for the polymer-stabilized SmC^*_α in which the appropriate temperature conditions for the polymerization reaction must be first determined. In our opinion, the SmC^*_α phase exists in pure form as long as two peaks are visible in the current response. These two peaks should be characterized by similar intensities and integrals. If the current response is different it may be caused by the influence of another phase which coexists with SmC^*_α or by external factors originating, e.g., from the geometry of measuring cells.

IV. SUMMARY

In this work, we have concentrated on the impact of polymer network on the thermodynamic stability of the SmC^*_α phase and its dynamic ability on switching under applying

time-dependent electric field. Using dielectric spectroscopy, polarizing microscopy, and differential scanning calorimetry, we have carefully characterized the neat liquid crystal of D16, which contains the SmC^*_α phase in a relatively wide temperature range and in liquid crystal-polymer system.

The results presented in this paper have shown that in D16 the SmC^*_α phase is located below the melting point and therefore we should classify this phase as unstable. Moreover, we have shown that the instability of SmC^*_α is related to the transformation to the crystalline phase. On the basis of our kinetic studies we were able to quantitatively evaluate the thermodynamic stability of neat D16.

We have successfully carried out the polymerization process with the addition of 5wt.% of the monomer to neat D16. As a result we have fabricated the PSD16 liquid crystal/polymer system. In this material the temperature range of the SmC^*_α phase was significantly shifted towards lower temperatures. The influence of the polymer network was also observed for other LC phases. For instance, in PSD16 we detected the coexistence of the SmC^* and crystalline phase. The former appears instead of the SmC^*_β phase. Unfortunately, after polymerization almost the same value of the melting temperature as for neat LC material was found. For this reason, after polymerization the SmC^*_α phase was still unstable. This observation indicates the difficulties to be overcome upon stabilization of the SmC^*_α phase by polymerization. Fortunately, the lifetime of the SmC^*_α phase specified at 46 °C is longer than that determined for neat D16 at the same temperature. Therefore we conclude that it is possible to improve thermodynamic stability of the LC material by formation of the polymer network within the SmC^*_α phase.

Detailed analysis of the temperature dependencies of permittivity in PSD16 system with respect to that observed in neat D16, reveals that the presence of the polymeric impurities suppresses the helix distortion mode, and as a consequence, a relative decrease in ε' is observed. It can be explained by interactions between polymer network and LC molecules which reduce the collective molecular fluctuations.

Because of the fuzzy phase transitions detected in the LC/polymer systems, in particular when a characteristic dielectric signature of SmC^*_α disappears after polymerization, the current reversal method (RCM) is proposed by us to identify the SmC^*_α phase. We claim that the pure SmC^*_α phase is detected by RCM as long as two peaks characterized by similar integral intensities and lying around to zero voltage are visible in the current response. If this characteristic response becomes gradually different from that described above as a function of temperature, it means that the influence of the neighboring phase is manifested and that the phase coexistence takes place. Despite obvious advantages of RCM, some limitations of this method appear even in neat LCs because of a similar current response from SmC^*_α, SmC^*_A, and/or de Vries smectics. Nevertheless, thanks to the dielectric measurements one can easily distinguish these smectic phases.

To sum up, only complementary use of both experimental techniques, i.e., dielectric spectroscopy and RCM, allows determination of the actual temperature range of the homogeneous SmC^*_α phase even in complex LC systems.

[1] S. Obayya, M. Farhat *et al.*, *Computational Liquid Crystal Photonics: Fundamentals, Modelling, and Applications* (Wiley, New York, 2016).

[2] C. C. Tartan, P. S. Salter *et al.*, J. Appl. Phys. **119**, 183106 (2016).

[3] J. Jiang, G. McGraw *et al.*, Opt Express **25**, 3327 (2017).

[4] B. Rezaei, I. H. Giden, and H. Kurt, Opt. Commun. **382**, 28 (2017).

[5] J. P. F. Lagerwall and F. Giesselmann, *Chiral Liquid Crystals*, Vol. 147 (Polish Academy of Sciences, Poznań, Poland, 2005).

[6] A. Labeeb, *The Rotational Viscosity and Field-Induced Transitions in the Intermediate Phases of Ferroelectric Liquid Crystals*, dissertation (University of Manchester, School of Physics and Astronomy, Manchester, England, 2011).

[7] A. Fukuda, Y. Takanishi, T. Isozaki, K. Ishikawa, and H. Takezoe, J. Mater. Chem. **4**, 997 (1994).

[8] A. Fafara, B. Gestblom, S. Wróbel, R. Dabrowski, W. Drzewiński, D. Kilian, and W. Haase, Ferroelectric **212**, 79 (1998).

[9] W. Drzewiński, R. Dąbrowski, K. Czupryński, J. Przedmojski, and M. Neubert, Ferroelectrics **212**, 281 (1998).

[10] I. Dierking, Materials **7**, 3568 (2014).

[11] P. Mach, R. Pindak, A. M. Levelut, P. Barois, H. T. Nguyen, H. Baltes, M. Hird, K. Toyne, A. Seed, J. W. Goodby, C. C. Huang, and L. Furenlid, Phys. Rev. E **60**, 6793 (1999).

[12] H. Takezoe, E. Gorecka, and M. Čepič, Rev. Mod. Phys. **82**, 897 (2010).

[13] B. Rovšek, M. Čepič, and B. Žekš, Phys. Rev. E **70**, 041706 (2004).

[14] V. P. Panov, N. M. Shtykov, A. Fukuda, J. K. Vij, Y. Suzuki, R. A. Lewis, M. Hird, and J. W. Goodby, Phys. Rev. E **69**, 060701(R) (2004).

[15] H. S. Chang, S. Jaradat, H. F. Gleeson, I. Dierking, and M. A. Osipov, Phys. Rev. E **79**, 061706 (2009).

[16] A. Labeeb, H. F. Gleeson, and T. Hegmann, Appl. Phys. Lett. **107**, 232903 (2015).

[17] H. Kikuchi, M. Yokota, Y. Hisakado, H. Yang, and T. Kajiyama, Nat. Mater. **1**, 64 (2002).

[18] J.-D. Lin, T.-Y. Wang, T.-S. Mo *et al.*, Sci Rep. **6**, 30407 (2016).

[19] P. Joshi, O Willekens, X Shang *et al.*, Photon. Lett. Poland **9**, 11 (2017).

[20] N. Rong, Y. Li, X. Li *et al.*, J. Display Technol. **12**, 1008 (2016).

[21] P. Archer and I. Dierking, J. Phys. D: Appl. Phys. **41**, 155422 (2008).

[22] J. Hoffmann, K. Nowicka, W. Kuczyński, and N. Bielejewska, Soft Mater **10**, 8548 (2014).

[23] K. Nowicka, M. Knapkiewicz, N. Bielejewska *et al.*, Liq. Cryst. **43**, 1778 (2016).

[24] M. J. Avrami, J. Chem. Phys. **7**, 1103 (1939).

[25] D. Vorländer, Z. Phys. Chem. **105**, 211 (1923).

[26] I. Dierking, Adv. Mater. **12**, 167 (2000).

[27] S. Kaur, I. Dierking, and H. F. Glesson, Eur. Phys. J. E. **30**, 265 (2009).

[28] N. Clark and S. T. Lagerwall, Appl. Phys. Lett. **36**, 899 (1980).

[29] Y. Takanishi, K. Hiraoka, V. K. Agrawal *et al.*, Jpn. J. Appl. Phys. **30**, 2023 (1991).

[30] A. Mikułko, M. Marzec, S. Wróbel, and R. Dąbrowski, Ferroelectrics **313**, 105 (2004).
[31] A. D. L. Chandani, T. Hagiwara, Y. Suzuki *et al.*, Jpn. J. Appl. Phys. **27**, L729 (1988).
[32] S. T. Lagerwall, *Ferroelectric and Antiferroelectric Liquid Crystals* (Wiley-VCH Verlag GmbH, New York, 1999), p. 383.
[33] J. P. F. Lagerwall, Phys. Rev. E **71**, 051703 (2005).
[34] E. Gorecka, D. Pociecha, M. Čepič, B. Žekš, and R. Dabrowski, Phys. Rev. E **65**, 061703 (2002).
[35] Y. Shen, L. Wang, R. Shao, T. Gong, C. Zhu, H. Yang, J. E. Maclennan, D. M. Walba, and N. A. Clark, Phys. Rev. E **88**, 062504 (2013).
[36] M. Zennyoji, J. Yokoyama, Y. Takanishi *et al.*, J. Appl. Phys. **37**, 6071 (1998).